



Characterization and cytotoxicity assessment of cadmium sulfide quantum dots synthesized with *Fusarium oxysporum f. sp. lycopersici*

Alexandra Calvo-Olvera¹ · Diana Issell Sandoval-Cárdenas² · Teresa García-Gasca³ · Aldo Amaro-Reyes² · Marcos De Donato-Capote⁴ · Norma Gabriela Rojas-Avelizapa¹

Received: 14 February 2023 / Revised: 25 May 2023 / Accepted: 31 May 2023 / Published online: 8 June 2023
© The Author(s), under exclusive licence to Springer-Verlag GmbH Germany, part of Springer Nature 2023

Abstract

The potential of CdS quantum dots for biomedical and bioimaging applications depends on their cytotoxicity, which can be modulated by coating molecules. Using sulfur as a precursor can be used along with cadmium nitrate to synthesize CdS quantum dots with the fungus *Fusarium oxysporum f. sp. lycopersici*. The latter replaces pure chemical sulfur as a precursor for CdS quantum dot synthesis, thus transforming waste into a value-added product, increasing sustainability, reducing the environmental impact of the process through the implementation of green synthesis techniques, and contributing to the circular economy. Therefore, we compared the cytotoxicity on HT-29 cells of biogenic, and chemical CdSQDs, synthesized by a chemical method using pure sulfur. Biogenic and chemical CdSQDs had diameters of 4.08 ± 0.07 nm and 3.2 ± 0.20 nm, Cd/S molar ratio of 43.1 and 1.1, Z-potential of -14.77 ± 0.64 mV and -5.52 ± 1.11 mV, and hydrodynamic diameters of 193.94 ± 3.71 nm and 152.23 ± 2.31 nm, respectively. The cell viability improved 1.61 times for biogenic CdSQDs over chemical CdSQDs, while cytotoxicity, measured as IC₅₀, diminished 1.88-times. The lower cytotoxicity of biogenic CdSQDs was attributed to their organic coating consisting of lipids, amino acids, proteins, and nitrate groups that interacted with CdS through -OH and -SH groups. Therefore, the biogenic synthesis of CdSQDs has repurposed a pathogenic fungus, taking advantage of the biomolecules it secretes, to transform hazardous sulfur waste and metal ions into stable CdSQDs with advantageous structural and cytotoxic properties for their potential application in biomedicine and bioimaging.

Keywords CdS quantum dots · Biogenic synthesis · Sulfur waste · Cytotoxicity · HT-29 cell line · *Fusarium oxysporum f. sp. Lycopersici*

Abbreviations

ATCC American type culture collection
ANOVA Analysis of variance

ICP-OES Inductively coupled plasma optical emission spectroscopy
C(-) biogenic Biogenic negative control
CB Biological control
CdSQDs Cadmium sulfide quantum dots
DMSO Dimethyl sulfoxide

Communicated by Yusuf Akhter.

✉ Norma Gabriela Rojas-Avelizapa
nrojasa@ipn.mx

Alexandra Calvo-Olvera
alexa.calvo1500@gmail.com

Diana Issell Sandoval-Cárdenas
issell.sandoval@uaq.edu.mx

Teresa García-Gasca
tggasca@uaq.edu.mx

Aldo Amaro-Reyes
aldo.amaro@uaq.edu.mx

Marcos De Donato-Capote
mdedonate@tec.mx

¹ Departamento de Biotecnología Ambiental, CICATA-Querétaro, Instituto Politécnico Nacional, Querétaro, México

² Planta Piloto de Biotecnología, Facultad de Química, Universidad Autónoma de Querétaro, Querétaro, México

³ Laboratorio de Biología Celular y Molecular, Facultad de Ciencias Naturales, Universidad Autónoma de Querétaro, Querétaro, México

⁴ Escuela de Ingeniería y Ciencias, Tecnológico de Monterrey, Querétaro, México

DMEM	Dulbecco's modified eagles' medium
DLS	Dynamic light scattering
EDS	Energy-dispersive X-ray spectroscopy
FBS	Fetal bovine serum
FTIR	Fourier-transform infrared spectroscopy
C(-) inorganic	Inorganic negative control
Hd	Hydrodynamic diameter
IC ₅₀	Inhibitory concentration 50%
MTT	3-(4,5-Dimethylthiazol-2-yl)-2,5-diphenyltetrazolium bromide
MGYP	Malt glucose yeast peptone media
CM	Medium control
% CV	Percentage of cell viability
PDI	Polydispersity index
PDA	Potato dextrose agar
QDs	Quantum dots
CPR	Reducing power control
TEM	Transmission electron microscopy

Introduction

Quantum dots (QDs) are semiconductor crystalline particles from groups II to VI or III to V, with sizes smaller than 10 nm, whose absorption and emission wavelengths are directly proportional to the QDs size (Javed et al. 2016; Abdellatif et al. 2022). This feature enables the development of QDs size-dependent applications, such as sensors and fluorophores for bioimaging (Javed et al. 2016). In contrast to organic photochromes, cadmium sulfide quantum dots (CdSQDs) are resistant to the photobleaching effect and have an extended luminescence lifetime; therefore, they can fluoresce for hours or days instead of a few seconds or minutes, and they are 20 times brighter and up to 100 times more stable (Chashchikhin and Budyka 2017; Mo et al. 2017). CdSQDs can be used for multicolor imaging because depending on their size, they emit different colors after excitation at one wavelength, which results in simultaneous color weathering. Moreover, because CdSQDs have narrow and symmetrical spectra, they do not overlap (Chashchikhin and Budyka 2017). CdSQDs can be conjugated with other biomolecules through functional groups on their surfaces, leading to highly sensitive molecular detection (Liang et al. 2021). Therefore, CdSQDs can be applied to in vivo and in vitro biolabeling, cellular imaging, diagnosis, surgical manipulation, photodynamic therapy, treatment of major diseases such as cancer, and as drugs themselves. The biomedical, bioimaging, and therapeutic applications depend on cytotoxicity (Javed et al. 2016; Liang et al. 2021).

Toxicological and stability issues that limit QDs use and development for diagnosis and therapy arise because most QDs are synthesized from heavy metals but they also depend on properties such as size, hydrodynamic diameter

(Hd), charge, coating molecules, and concentration (Javed et al. 2016; Chashchikhin and Budyka 2017; Abdelbasir and Shalan 2019; Harish et al. 2020). Naked CdSQDs have been reported to be toxic because Cd²⁺ binds to thiol groups, mainly on mitochondrial molecules, generating stress and damage leading to cell death (Mo et al. 2017). In addition, the chemical synthesis of QDs could use toxic reducing agents that would persist within the final product (Abdellatif et al. 2022). The cytotoxicity of naked CdSQDs can be diminished by the addition of surface coatings (Harish et al. 2020), such as glutathione, thus enabling their use in biomedical applications. Biogenic synthesis of QDs decreases the use of toxic agents, with up to 90% transformation efficiency, and the production of coated QDs with biomolecules such as proteins, thus leading to higher biocompatibility, stability in aqueous solutions, and considerable resistance to evaporation (Mo et al. 2017; Qin et al. 2018).

Biogenic synthesis of QDs can be carried out using plant extracts, bacteria, or fungi. In contrast to plant-based synthesis, fungal biosynthesis does not require expensive downstream processing to obtain alcoholic extracts, which are then used for nanoparticle synthesis (Subramaniam et al. 2022). Bacterial and fungal biosynthesis yields QDs intra- or extra-cellularly. Fungi are easily cultivated and yield CdSQDs mainly extracellularly because the metal ions trapped on the cellular surface are enzymatically reduced and mycelia can be simply removed through filtration, thus reducing production costs (Sandoval-Cárdenas et al. 2017a, b; Xu et al. 2019). This contrasts with the intracellular biosynthesis of QDs with bacteria, where a lysis process is required to release the product, thus increasing production costs.

Nowadays, the use of a circular economy is necessary for new developments, and transforming waste into new products is an option to achieve this, and doing so through green processes is encouraged to reduce the pollution derived from waste generation (Figge et al. 2023). The Mexican oil industry produces sulfur waste, which is removed from oil through the Claus process and is finally classified as a toxic waste that must be properly disposed (Spatolisano et al. 2022). However, this sulfur residue is nearly pure; therefore, it can be used along with cadmium nitrate to biosynthesize CdSQDs with the fungus *Fusarium oxysporum f. sp. lycopersici* (Sandoval-Cárdenas et al. 2017b). The biosynthesized CdSQDs are a value-added product that now forms part of the circular economy, as they were obtained using green synthesis techniques where the sulfur residue replaced chemical precursors (Abdelbasir et al. 2020; Figge et al. 2023). In addition, this biosynthesis repurposes the phytopathogenic fungus *F. oxysporum f. sp. lycopersici*, taking advantage of its simple cultivation and its ability to secrete a large number of enzymes, which are mainly responsible for the reduction processes of the metal ions, yielding

QDs, affecting the reaction equilibrium, particle nucleation, and growth rates, and thus influencing particle size, shape, and coating biomolecules leading to increased QDs stability (Guilger-Casagrande and Lima 2019). *F. oxysporum f. sp. lycopersici* is also tolerant to environments contaminated with hydrocarbons, pesticides, and heavy metals and has been used for the production of nanomaterials of various compounds that other microorganisms would not tolerate (Rai et al. 2021). It has been reported that *Fusarium oxysporum f. sp. lycopersici* is able to biosynthesize silver, gold, cadmium sulfide, platinum, and zirconium nanoparticles; however, very little is known about the biomolecules involved in the process (Pourali et al. 2018; Gupta and Chundawat 2019). The cytotoxicity of the biosynthesized CdSQDs with *F. oxysporum f. sp. lycopersici* from CdSO₄ and the sulfur waste recovered from oil desulfurization (Sandoval-Cárdenas et al. 2017b) still needs to be assessed to enable their use in biomedical applications.

The present study aimed to compare the cytotoxicity of chemical and biogenic CdSQDs in vitro, in human colorectal adenocarcinoma cells HT-29. The sulfur residue from the petrochemical industry was used as the precursor for the assembly of biogenic CdSQDs, potentially conferring added value to this waste. The CdSQDs were characterized by UV-visible, Energy-Dispersive X-ray Spectroscopy (EDS), Transmission Electron Microscopy (TEM), X-ray Spectroscopy, Dynamic Light Scattering (DLS), and Fourier-Transform Infrared Spectroscopy (FTIR).

Materials and methods

Materials

The sulfur waste recovered from a Claus reaction unit for oil desulfurization was provided by the Mexican Petroleum Institute. The fungus *Fusarium oxysporum f. sp. lycopersici* 4287 was provided by the PhD. Macias-Sánchez (UPIIG-IPN). The human colorectal adenocarcinoma cell line HT-29 ATCC® (HTB-38™) (American Type Culture Collection, Rockville, CT, USA) was provided by the PhD Teresa García-Gasca (Cellular and Molecular Biology Laboratory at the Autonomous University of Queretaro). Na₂S, Cd(NO₃)₂, ethanol, Dulbecco's modified Eagle's medium (DMEM) and Fetal Bovine Serum (FBS) were purchased from Sigma-Aldrich (USA). The MGYP and antibiotic-antimycotic were obtained from Gibco (USA).

Synthesis of biogenic CdSQDs

The biomass of *Fusarium oxysporum f. sp. lycopersici* was used to produce of biogenic CdSQDs, as previously reported by Sandoval et al. (2017a, b) and Calvo-Olvera et al. (2021).

The fungus was grown in Potato Dextrose Agar (PDA) at 30 °C for 72 h, followed by addition of 0.8% (w/v) NaCl to retrieve the conidia. Then, 30 mL of sterile MGYP (g/L: 3 malt extract, 10 glucose, 3 yeast extract, and 5 peptone) was inoculated to 1 × 10⁵ spores/mL and incubated for 4 days at 30 °C and 150 rpm. Afterwards, the biomass was recovered in Whatman No. 4 paper by vacuum filtration, rinsed thrice with sterile distilled water, and 6 g of biomass were incubated with 62.5 mL of sterile 1 mM Cd(NO₃)₂ and 0.62 g of sulfur residue for 12 h at 30 °C and 150 rpm. An inorganic negative control [C(-) inorganic] was assembled as a mixture of 62.5 mL with 1 mM Cd(NO₃)₂ and 0.62 g of sulfur residue. The biogenic negative control [C(-) biogenic] consisted of 6 g of biomass in 62.5 mL of sterile deionized water. Both controls were incubated as previously described. The medium containing QDs was centrifuged at 10,000 rpm for 10 min and filtered with a 0.22 μm cellulose membrane to eliminate residual biomass and sulfur. The samples were stored at 4 °C until use. Water from the CdSQDs was evaporated at 50 °C to preserve the components necessary for biological stabilization. The dried material was seeded in MGYP agar medium, incubated for 4 days at 28 °C, and observed under an AxioScope A1 bright-field optical microscope (Zeiss, Germany) to verify sterility.

Chemical synthesis of CdSQDs

The chemical CdSQDs were prepared using the methodology described by Khan et al. (2011). Briefly, 50 mL of 0.1 M Na₂S was mixed with 50 mL of 0.1 M Cd(NO₃)₂ at 10,000 rpm for 10 min. The precipitate was washed three times with 5 mL ethanol 96% (v/v) and centrifuged at 10,000 rpm for 10 min. Finally, the QDs were dried at 70 °C for 4 h.

CdSQDs characterization

The structural and elemental composition of CdSQDs were characterized. The shape and size of the CdSQDs were observed using Transmission Electron Microscopy (TEM). The aqueous samples were ultrasonicated at 130 W, 20 kHz and 50% amplitude for 15 min. A drop was then placed on a holey carbon copper grid and dried at room temperature for 24 h. TEM analysis was performed at 80 kV and 200,000× using a JEOL JEM-1010, USA. The diameters of at least 200 particles were measured using Image J V 1.8.0. The samples were sonicated for 15 min and a drop was placed on a Cu-lacey rack and dried at room temperature for 12 h. Subsequently the elemental composition was determined by EDS in X-Max equipment (Oxford Instruments, UK) using a JSM 7800F scanning electron microscope (JEOL, USA) with a beam of 16 kV electrons. DLS was carried out three times with a Litesizer 500 (Anton Paar, AUS),

samples were sonicated for 10 min and a tenfold dilution was prepared with injectable water for analysis. The functional groups on the surface of C(-) biogenic, biogenic, and chemical CdSQDs were identified by FTIR analysis using Cary 670 equipment (Agilent Technologies, USA) operated with a 4 cm⁻¹ resolution, within 500 to 4000 cm⁻¹.

In vitro cytotoxicity assessment

HT-29 cells, a colon cancer cell line, were cultivated in DMEM supplemented with 10% (w/v) FBS and antibiotic–antimycotic (100 U/mL penicillin, 100 µg/mL streptomycin, and 0.25 µg/mL amphotericin B), and incubated at 37 °C in a humidified atmosphere with 5% (v/v) CO₂ until a cellular confluence of over 80% was achieved. Next, 1 × 10⁴ cells/well were seeded in a 96-well tissue culture plate and incubated for 24 h under the same conditions. Cytotoxicity was assessed by adding 100 µl of 1, 5, 10, or 100 µg CdSQDs/mL of biogenic or chemical CdSQDs into the wells containing cells, and they were incubated for 24 h under the same conditions. The negative control (C-) consisted of untreated cells, whereas 1 mM H₂O₂ was added to the positive control (C+). Control of reducing power (CRP) consisted of DMEM-SFB medium with 100 µl of biogenic or chemical CdSQDs at a concentration of 100 µg/mL, and the CRP control was performed to evaluate whether there was any interference in the reduction of MTT by the NPs by itself. Finally, 100 µl of 100 µg/mL fungal biomass was added to the biological control (CB), and this control was performed to evaluate whether there was any cytotoxicity due to the biomass. Three replicates were used for each experiment.

After exposure to CdSQDs, cellular proliferation and survival were measured using a 3-(4,5-dimethylthiazol-2-yl)-2,5-diphenyltetrazolium bromide (MTT) assay. Twenty µl of MTT was added to the wells and incubated for 1 h at 37 °C in a humidified atmosphere containing 5% (v/v) CO₂. The supernatant was removed and 100 µl of dimethyl sulfoxide (DMSO) was added to each well and incubated for 10 min. The absorbance of each sample at 570 nm (A₅₇₀) was measured using a SPECTROmax 250 spectrophotometer (Molecular Devices, USA). The percentage of cell viability (CV %) was determined using the mean values of A₅₇₀ as the coefficient of Eq. (1).

$$CV (\%) = \frac{\text{Mean } A_{570} \text{ sample} - \text{Mean } A_{570} \text{ medium control}}{\text{Mean } A_{570} \text{ negative control} - \text{Mean } A_{570} \text{ medium control}} \times 100, \quad (1)$$

The half-maximal inhibitory concentration (IC₅₀) was determined by extrapolation from the cell viability percentage against the CdSQDs concentration, using GraphPad Prism software version 9.

Statistical analysis

Three replicates of each test were performed. The results are expressed as mean ± standard deviation. The size, Hd, and z-potential of the chemical and biogenic CdSQDs were compared using Tukey's test. The MTT was analyzed using two-way analysis of variance (ANOVA) followed by Tukey's test. Statistical significance was set at $P < 0.05$. The MTT results were analyzed using GraphPad Prism software version 9.

Results and discussion

Characterization of QDs

The UV–vis absorption spectra obtained from both samples were previously reported by Calvo-Olvera et al. (2021a) and Sandoval-Cárdenas et al. (2017a, b), where the biogenic CdSQDs showed bands at 230, 260, and 320 nm. The first band was attributed to the presence of tyrosine (Saraiva 2020), phenols, nucleic acids (Shen 2019), and carbohydrates. The second band is due to the presence of NADPH, NADH, glutathione, and aromatic amino acids (Sandoval-Cárdenas et al. 2017b), and the third band is for biogenic CdSQDs (Sandoval-Cárdenas et al. 2017a, b). The chemical CdSQDs showed absorption bands at 230 and 440 nm. The first band was also observed in the C(-) chemical spectrum, and the second band showed the presence of CdSQDs (Calvo-Olvera et al. 2021).

Transmission electron microscopy (TEM)

The micrographs obtained by TEM analysis of biogenic and chemical CdSQDs are shown in Fig. 1. Both CdSQDs showed spheroid-agglomerated particles under 10 nm in size; therefore, they can be categorized as QDs. Biogenic CdSQDs had bigger sizes but a narrower dispersion than chemical CdSQDs, they had significantly different average diameters of 4.08 ± 0.07 nm and 3.2 ± 0.20 nm, respectively. The biogenic CdSQDs formed amorphous aggregates, whereas the chemical CdSQDs formed elongated geometrical aggregates. Comparable crystal structures for the latter were reported by Dey et al. (2020). Qin et al. (2018), who synthesized elongated CdS nanocrystals by a

similar synthesis procedure, attributing these formations to the water added in the process. On the other hand, when the QDs precursors are depleted and the synthesis process continues, the nanoparticles were crowded and tended to

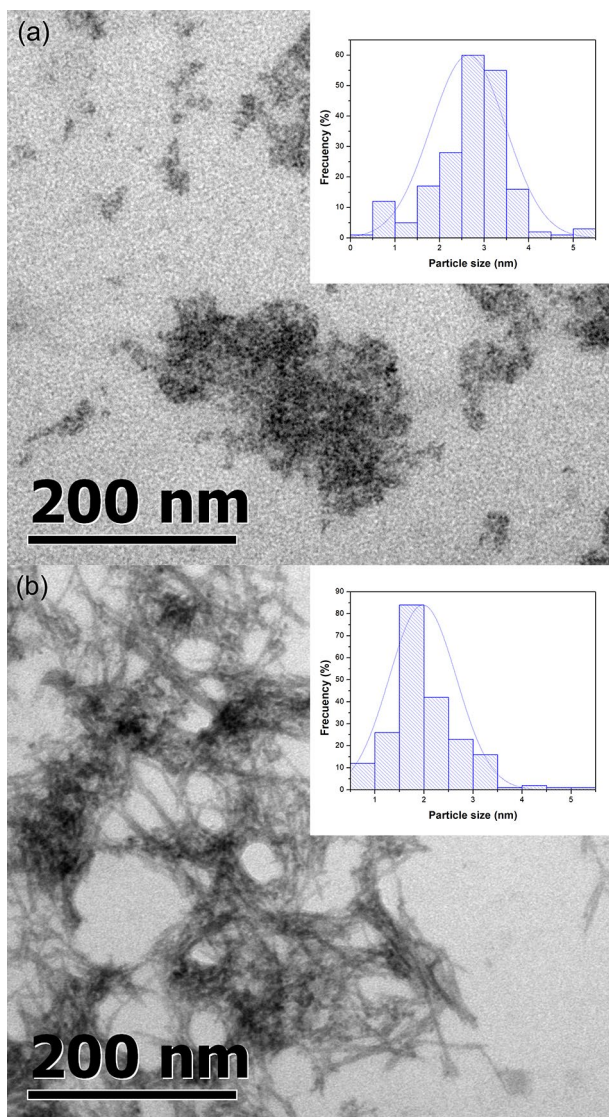


Fig. 1 TEM micrographs of **a** biogenic and **b** chemical CdSQDs. The insets show the size distribution histograms

join, leading to large and irregular CdS crystals, so the formation of these structures could be due to the duration of the reaction (Alkhayattomran and Ahmed 2021). Here, the differences in aggregate structure between the chemical and biogenic CdSQDs could be attributed to differences in the stabilizing agents.

The diameters of the chemical CdSQDs were similar to those reported by other authors for chemical syntheses. Yadav et al. (2019) synthesized spherical CdSQDs of 2.3 nm via wet chemical method. Yang et al. (2018), synthesized CdSQDs coated with N-acetyl-L-cysteine and Mn with sizes ranging from 3.5 to 2.9 nm, and Arunadevi et al. (2015), used a similar procedure with increased temperature and found a positive correlation between temperature and particle size, obtaining CdSQDs of 4.5 nm

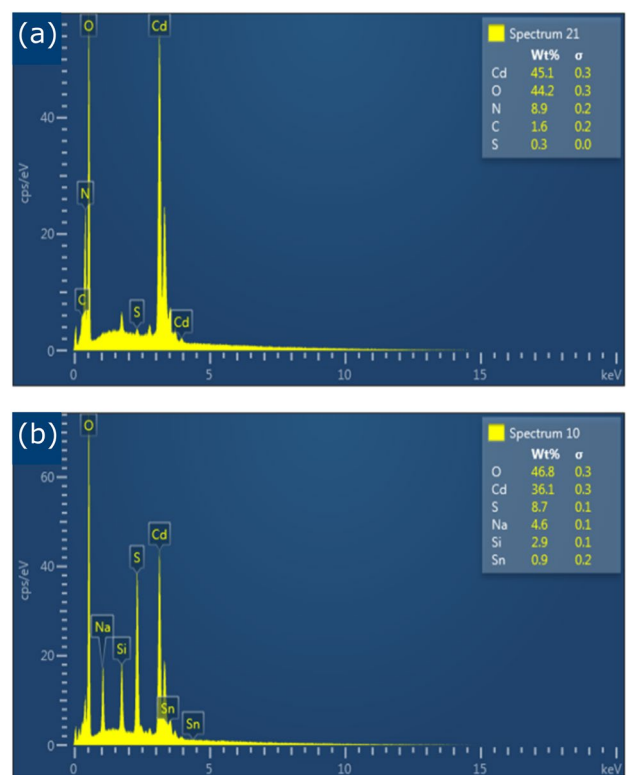


Fig. 2 Energy dispersive spectra of **a** biogenic CdSQDs and **b** chemical CdSQDs. The insets show the percentage composition of the analyzed samples

at 20 °C. However, CdS crystals have not been reported in the above cases.

Biogenic QDs have diameters and shapes similar to those of QDs synthesized with other microorganisms. Several authors have biosynthesized CdSQDs with related diameters; Sakpirom et al. (2019), obtained spherical particles of 4.85 nm with *Rhodospseudomonas palustris*; Alsaggaf et al. (2020), produced 2–10 nm QDs with *Aspergillus niger*; Gallardo-Benavente et al. (2019), produced QDs of 2 and 16 nm by the antarctic strain *Pseudomonas fragi* CG01; and Qin et al. (2018), 6 nm with *Trametes versicolor*.

EDS analysis

The elements present in the solution containing the QDs were identified using EDS. The EDS spectra of biogenic and chemically synthesized QDs are shown in Fig. 2a and b, respectively. Both the QDs contained Cd, S and O. The Cd/S molar ratio was 43.1 for biogenic and 1.1 for chemical CdSQDs, which suggests that biogenic CdSQDs have a Cd core surrounded by sulfur or S-containing groups, while chemical CdSQDs have a similar amount of both elements. This ratio could explain the increased size observed in the TEM analysis of biogenic compared

to chemical CdSQDs. The presence of O, N, and C in biogenic CdSQDs was attributed to biomolecules that participate in QDs synthesis and stabilization. Oxygen has been attributed to the aeration of the fungal mycelium in an aqueous medium (Gallardo-Benavente et al. 2019), and nitrogen comes from the $\text{Cd}(\text{NO}_3)_2$ used for the synthesis. Other authors have observed the appearance of oxygen peaks due to carboxylates on the surface of the QDs (Gallardo-Benavente et al. 2019). Concerning chemical QDs, sodium comes from the Na_2S used for their synthesis, whereas Si and Sn could be attributed to impurities in the mixture.

DLS analysis

DLS was employed to measure aggregation, Z-potential, Hd, and polydispersity index (PDI). The Z-potential for biogenic and chemical CdSQDs was -14.77 ± 0.64 mV and -5.52 ± 1.11 mV, respectively; the Tukey test showed significant differences among samples. The negative charge of biogenic CdSQDs could be due to specific biomolecules, such as negatively charged amino acids or cysteine (Gallardo-Benavente et al. 2019), whereas the negative charge of chemical CdSQDs was attributed to a double electrical layer of nitrate (Khan et al. 2011). The Z-potentials of both colloidal systems suggest instability; however, biogenic CdSQDs were more stable than chemical CdSQDs were.

The mean value of hydrodynamic diameter (Hd) for the biogenic CdSQDs was 193.94 ± 3.71 nm with a PDI of 0.01; for chemical CdSQDs it was 152.23 ± 2.31 nm with a PDI of 0.01, which was significantly different ($P < 0.05$). The larger size of biogenic CdSQDs could be attributed to the larger biomolecules that coated the QDs (Siddiqi et al. 2018). The organic coating also influenced their agglomeration and stability; the biogenic CdSQDs showed no precipitation, which agrees with the Z-potential data.

Hd analysis suggested that both QDs had a coating layer. No differences were observed among the PDI of the QDs, indicating sample uniformity. The PDI values indicated that QDs were monodisperse, since their values were under 0.1 (Danaei et al. 2018). The Hd of CdSQDs was larger than the size shown by TEM analysis because DLS measures not only the QDs but also the dipole electric charge attached to their surface. When a particle moves in a liquid medium, a dipole electric charge attaches and modifies the motion of the particle; the size determined by the latter technique is larger, suggesting an organic coating for biogenic CdSQDs and electrostatic charge stabilization for chemical CdSQDs. The agglomeration of QDs shown in TEM images could also be detected using DLS equipment.

FTIR analysis

The composition of the QDs surface was analyzed using FTIR. Figure 3b and c show the spectra obtained for biogenic and chemical CdSQDs, respectively. The extracellular filtrate of *F. oxysporum*, which was used as a negative control for biogenic QDs, is shown in Fig. 3a. The biogenic CdSQDs and negative control showed absorption peaks at 1625, 1552, 1406, 1237, and 670 cm^{-1} , which demonstrated the presence of coating biomolecules on the surface of the biogenic QDs. The absorbance peak at 1625 cm^{-1} was attributed to lipids, and the peak at 1406 cm^{-1} was attributed to the carboxyl groups of amino acids and $-\text{CH}_2$ of lipids (Fígoli et al. 2017). The peak at 1552 cm^{-1} indicated the presence of amide I and II bonds in proteins of the *Fusarium* genus (Forfang et al. 2017), and the peak at 1237 cm^{-1} indicated C–O–C stretching in esters and nitrate groups (Naranthatta et al. 2021). Biogenic CdSQDs showed a peak at 3216 cm^{-1} which was attributed to the stretching of the $-\text{OH}$ group due to water on the surface of the CdSQDs. The peak at 614 cm^{-1} corresponded to the vibrations of Cd–S stretching (Murugesan et al. 2018). The peaks in the range of $400\text{--}1000\text{ cm}^{-1}$ were due to the phonons of the second harmonic of CdS and the C–S vibration of the thiol group coordinated with the surface

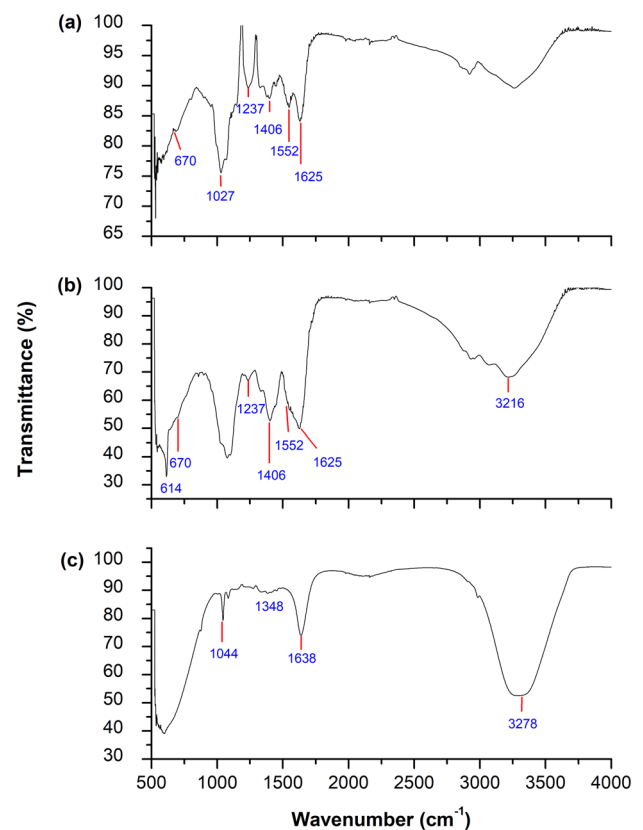


Fig. 3 FTIR spectrum **a** *F. oxysporum* biomass, **b** biogenic CdSQDs, and **c** chemical CdSQDs

of the particle (Carrasco et al. 2021). The negative control spectra showed a peak at 1027 cm^{-1} due to C–O bond carbohydrates (Forfang et al. 2017) and glycogen (Javed et al. 2016) of the *Fusarium* genus. The chemical CdSQDs spectra showed a peak at 1273 cm^{-1} attributed to the nitrate groups; peaks at 1638 and 1384 cm^{-1} corresponded to carboxylates with asymmetric and symmetric stretching modes, respectively; the peak at 3278 cm^{-1} has been reported for water molecules; and the peak at 1044 cm^{-1} was due to the flexion mode of CH (Karatop et al. 2022).

Cytotoxicity assessment

The viability of HT-29 cells was measured by MTT assay, in which the mitochondrial enzymes reacted with MTT and produced a purple-colored formazan product, and the quantity of formazan produced was directly proportional to the number of viable cells (Karatop et al. 2022). The cell viability results for both types of QDs are shown in Fig. 4. The cell viability was dose-dependent and decreased as the concentration of biogenic or chemical QDs increased. Treatment with $1\text{ }\mu\text{g/mL}$ of biogenic and chemical CdSQDs reached 65.2% and 44% of cell viability, while treatments with $100\text{ }\mu\text{g/mL}$ showed 22.9% and 14.22% cell viability, respectively, this meant a 1.48 and 1.61-fold increase. Cell viability was higher in samples treated with biogenic CdSQDs at all the evaluated concentrations, except at $5\text{ }\mu\text{g/mL}$, where no significant difference ($P < 0.05$) was found. These results indicate cytotoxicity modulation through biomolecules on the surface of the biogenic CdSQDs. It has been shown that the coatings on the surface of QDs mediate cell interactions, such as internalization and cell wall binding; they also increase the stability of QDs. The amino acids present in the coating of QDs, such as Tyr and Trp, reduce the exposed ions through their phenol and indole groups (Gupta 2019; Matur et al. 2020). The IC_{50} , which is

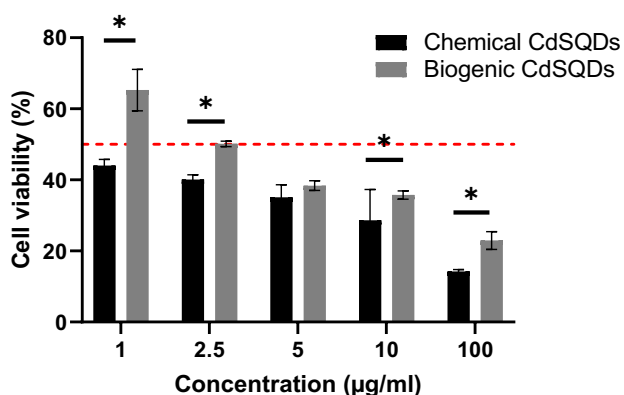


Fig. 4 Cell viability resulting from MTT assay of HT-29 cells treated with biogenic CdSQDs (grey) and chemical CdSQDs (black) (mean \pm SD, $n = 3$). *Statistical difference between groups ($p < 0.05$)

the concentration that causes 50% inhibition in a population, was $3.02\text{ }\mu\text{g/mL}$ and $1.6\text{ }\mu\text{g/mL}$ for the biogenic and chemical CdSQDs, respectively. Chemical CdSQDs had almost twice the cytotoxicity compared to biogenic CdSQDs, which was attributed to the presence of biomolecules covering the surface of biogenic QDs, thus preventing the direct contact of CdS with cell membranes and organelles. This coating of biomolecules might also prevent the release of Cd ions, which form ionic and covalent bonds with intracellular cell components leading to cell death; therefore, the biomolecules coating QDs achieved the protection of cell structures (Dabhane et al. 2021). Shell QDs and biogenic QDs have been shown to have reduced to no cytotoxicity, because the surface ligands on the QDs limit the transport of oxygen, thus decreasing cell oxidation (Pikula et al. 2020).

The cytotoxicity of distinct types of CdSQDs depends on several characteristics such as shape, coating, and surface charge (Sukhanova et al. 2022). The higher toxicity of the chemical CdSQDs can also be attributed to the cadmium crystals observed in Fig. 1b. Tubular or thread forms have been reported to exhibit higher cytotoxicity owing to their surface reactivity, inducing oxidative stress and inflammatory processes (Matos et al. 2020). Smaller QDs exhibit increased toxicity because they can penetrate the cell membrane and reach the nucleus (Shivashankarappa and Sanjay, 2020). Toxicity also depends on the organism, cell line, CdSQDs concentration, exposure time, and culture media (Sukhanova et al. 2022). However, some reports have shown low toxicity of QDs synthesized by biological methods or employing polymer-coated QDs. A similar IC_{50} of $4\text{ }\mu\text{g/mL}$ for the HELA cell line was reported by Hossain and Mukherjee (2013). The IC_{50} values were smaller than those described by Reyes-Esparza et al. (2015), who reported IC_{50} values of 5 and $6\text{ }\mu\text{g/mL}$ for HepG2 and HEK293, respectively. These differences in cytotoxicity among cell lines were also observed by Shivashankarappa and Sanjay (2020), who reported IC_{50} of 92.2 and 33.4 mM for B16F10 and A431 cell lines respectively, when applying CdSQDs synthesized by *E. coli*. Harish et al. (2020), assessed the cytotoxicity in Vero cells with CdSQDs covered with polyvinylpyrrolidone (PVP) and cysteine. They found that the cells treated with modified CdSQDs had increased viability at all concentrations, obtaining 40% of cell viability with $1\text{ }\mu\text{g/mL}$ of cysteine coated CdSQDs; a similar result was observed in this work. Calvo-Olivera et al. (2021a), evaluated the same type of biogenic and chemical QDs on sprouts of *Lactuca sativa* plants and *E. coli* and found that the chemical QDs inhibited *E. coli* proliferation at all concentrations tested, but the biogenic QDs only showed antibacterial activity at the highest concentration, and did not inhibit seed germination.

The sulfur residue was analyzed by Inductively Coupled Plasma Optical Emission Spectroscopy (ICP-OES) to analyze the metal content, as reported by Sandoval-Cárdenas

et al. (2017b), which was shown to contain Fe, Mg, and Al, revealing high purity and the absence of heavy metals; therefore, the use of this residue does not pose a health risk.

Conclusion

Both biogenic and chemical synthesis can produce spherical, monodisperse, and mildly stable CdSQDs. Biogenic synthesis of CdSQDs leads to an increased Cd/S molar ratio; the increased Hd was due to the addition of coating biomolecules such as lipids, amino acids, and proteins with thiol groups. The presence of nitrate carboxylates and -CH groups on the surface of the chemical CdSQDs had a smaller effect on Hd. The coating molecules obtained through biogenic synthesis increased the cell viability and reduced cytotoxicity of CdSQDs.

Therefore, we can conclude that biogenic synthesis from petroleum sulfur residues provides CdSQDs with structural characteristics that are advantageous for their potential application in biomedicine and bioimaging when compared to those obtained by chemical synthesis. The phytopathogenic fungus *F. oxysporum f. sp. lycopersici* was repurposed to yield stable CdSQDs.

However, it is still necessary to evaluate the cytotoxicity mechanisms caused by biogenic CdSQDs in cells and to compare them with the mechanisms caused by chemical CdSQDs, as the lack of coating molecules may facilitate their entry into the cell, whereas biogenic CdSQDs may interact with the cell wall, thereby diminishing their cytotoxicity.

Supplementary Information The online version contains supplementary material available at <https://doi.org/10.1007/s00203-023-03604-x>.

Author contributions All the authors contributed to the conception and design of the study. AC and DS contributed evenly as first authors. Conceptualization: AC and DS. Methodology: AC. Funding acquisition: NR, DS, TG. Writing original draft: AC and DS. Writing-review and editing: DS, NR, TG, AA and MD. Supervision: DS, NR, TG and MD. All authors have read and approved the final manuscript.

Funding This research was funded by Grant A1-S-31777 of the Consejo Nacional de Ciencia y Tecnología (CONACYT), Instituto Politécnico Nacional, and Universidad Autónoma de Querétaro.

Data availability The datasets generated and/or analyzed during the current study are available from the corresponding author upon reasonable request.

Declarations

Conflict of interest The authors declare that they have no conflicts of interest.

Ethical approval This research does not require ethics approval, as it is not involved in human or animal studies.

Consent to participate Informed consent was obtained from all individual participants included in the study.

References

- Abdelbasir SM, Shalan AE (2019) An overview of nanomaterials for industrial wastewater treatment. *Korean J Chem Eng* 36:1209–1225. <https://doi.org/10.1007/s11814-019-0306-y>
- Abdelbasir SM, McCourt KM, Lee CM, Vanegas DC (2020) Waste-derived nanoparticles: synthesis approaches, environmental applications, and sustainability considerations. *Front Chem* 8:782. <https://doi.org/10.3389/FCHEM.2020.00782/BIBTEX>
- Abdellatif AhAH, Tawfeek HM, Younis MA et al (2022) Biomedical applications of quantum dots: overview, challenges, and clinical potential. *Int J Nanomed* 17:1951–1970. <https://doi.org/10.2147/IJN.S357980>
- Alkhayattomran AH, Ahmed MR (2021) Impact of reaction temperature on the structural, surface morphology and antibacterial activity of hydrothermally synthesized CdS nanoparticles. *J Phys Conf Ser* 1879:032091. <https://doi.org/10.1088/1742-6596/1879/3/032091>
- Alsaggaf MS, Elbaz AF, El BS, Moussa SH (2020) Anticancer and antibacterial activity of cadmium sulfide nanoparticles by *aspergillus niger*. *Adv Polym Technol* 2020:1–13. <https://doi.org/10.1155/2020/4909054>
- Arunadevi R, Latha M, Velumani S et al (2015) Synthesis and characterization of cadmium sulfide nanoparticles by chemical precipitation method. *J Nanosci Nanotechnol* 15:8434–8439. <https://doi.org/10.1166/JNN.2015.11472>
- Calvo-Olvera A, De Donato-Capote M, Pool H, Rojas-Avelizapa NG (2021) In vitro toxicity assessment of fungal-synthesized cadmium sulfide quantum dots using bacteria and seed germination models. *J Environ Sci Health A* 56:713–722. <https://doi.org/10.1080/10934529.2021.1899718>
- Carrasco V, Amarelle V, Lagos-Moraga S et al (2021) Production of cadmium sulfide quantum dots by the lithobiotic Antarctic strain *Pedobacter* sp. UYPI and their application as photosensitizer in solar cells. *Microb Cell Fact* 20:1–10. <https://doi.org/10.1186/S12934-021-01531-4/TABLES/1>
- Chashchikhin OV, Budyka MF (2017) Photoactivation, photobleaching and photoetching of CdS quantum dots—Role of oxygen and solvent. *J Photochem Photobiol A Chem* 343:72–76. <https://doi.org/10.1016/J.JPHOTOCHEM.2017.04.028>
- Dabhane H, Ghotekar S, Tambade P et al (2021) A review on environmentally benevolent synthesis of CdS nanoparticle and their applications. *Environ Chem Ecotoxicol* 3:209–219. <https://doi.org/10.1016/J.ENCECO.2021.06.002>
- Danaei M, Dehghankhold M, Ataei S et al (2018) Impact of particle size and polydispersity index on the clinical applications of lipidic nanocarrier systems. *Pharmaceutics* 10:57. <https://doi.org/10.3390/pharmaceutics10020057>
- Dey PC, Sarkar S, Das R (2020) X-ray diffraction study of the elastic properties of jagged spherical CdS nanocrystals. *Mater Sci* 38:271–278. <https://doi.org/10.2478/msp-2020-0032>
- Figge F, Thorpe AS, Gutberlet M (2023) Definitions of the circular economy: circularity matters. *Ecol Econ* 208:107823. <https://doi.org/10.1016/J.ECOLECON.2023.107823>
- Fígoli CB, Rojo R, Gasoni LA et al (2017) Characterization of *Fusarium graminearum* isolates recovered from wheat samples from Argentina by Fourier transform infrared spectroscopy: phenotypic diversity and detection of specific markers of aggressiveness. *Int J Food Microbiol* 244:36–42. <https://doi.org/10.1016/J.IJFOODMICRO.2016.12.016>

- Forfang K, Zimmermann B, Kosa G et al (2017) FTIR spectroscopy for evaluation and monitoring of lipid extraction efficiency for oleaginous fungi. *PLoS One* 12:e0170611. <https://doi.org/10.1371/JOURNAL.PONE.0170611>
- Gallardo-Benavente C, Carrión O, Todd JD et al (2019) Biosynthesis of cds quantum dots mediated by volatile sulfur compounds released by antarctic pseudomonas fragi. *Front Microbiol* 10:1866. <https://doi.org/10.3389/FMICB.2019.01866/BIBTEX>
- Guilger-Casagrande M, de Lima R (2019) Synthesis of silver nanoparticles mediated by fungi: a review. *Front Bioeng Biotechnol*. <https://doi.org/10.3389/fbioe.2019.00287>
- Gupta R (2019) Cadmium nanoparticles and its toxicity. *J Crit Rev* 6:1–7
- Gupta K, Chundawat TS (2019) Bio-inspired synthesis of platinum nanoparticles from fungus *Fusarium oxysporum*: its characteristics, potential antimicrobial, antioxidant and photocatalytic activities. *Mater Res Express* 6:1050d6. <https://doi.org/10.1088/2053-1591/ab4219>
- Harish R, Nisha KD, Prabakaran S et al (2020) Cytotoxicity assessment of chitosan coated CdS nanoparticles for bio-imaging applications. *Appl Surf Sci* 499:143817. <https://doi.org/10.1016/J.APSUSC.2019.143817>
- Hossain ST, Mukherjee SK (2013) Toxicity of cadmium sulfide (CdS) nanoparticles against *Escherichia coli* and HeLa cells. *J Hazard Mater* 260:1073–1082. <https://doi.org/10.1016/J.JHAZMAT.2013.07.005>
- Javed H, Fatima K, Akhter Z et al (2016) Fluorescence modulation of cadmium sulfide quantum dots by azobenzene photochromic switches. *Proc R Soc A Math Phys Eng Sci*. <https://doi.org/10.1098/RSPA.2015.0692>
- Karatop EU, Cimenci CE, Aksu AM et al (2022) Colorimetric cytotoxicity assays. *Cytotox*. <https://doi.org/10.5772/INTEC.HOPEN.105772>
- Khan ZR, Zulfequar M, Khan MS (2011) Chemical synthesis of CdS nanoparticles and their optical and dielectric studies. *J Mater Sci* 46:5412–5416. <https://doi.org/10.1007/S10853-011-5481-0/FIGURES/7>
- Liang Z, Khawar MB, Liang J, Sun H (2021) Bio-conjugated quantum dots for cancer research: detection and imaging. *Front Oncol* 11:4300. <https://doi.org/10.3389/FONC.2021.749970/BIBTEX>
- Matos B, Martins M, Samamed AC et al (2020) Toxicity evaluation of quantum dots (ZnS and CdS) singly and combined in zebrafish (*Danio rerio*). *Int J Environ Res Public Heal* 17:232. <https://doi.org/10.3390/IJERPH17010232>
- Matur M, Madhyastha H, Shruthi TS et al (2020) Engineering bioactive surfaces on nanoparticles and their biological interactions. *Sci Rep* 10(10):1–14. <https://doi.org/10.1038/s41598-020-75465-z>
- Mo D, Hu L, Zeng G et al (2017) Cadmium-containing quantum dots: properties, applications, and toxicity. *Appl Microbiol Biotechnol* 101(10):2713–2733. <https://doi.org/10.1007/S00253-017-8140-9>
- Murugesan R, Sivakumar S, Karthik K et al (2018) Issue 3 www.jetir.org (ISSN-2349-5162). *JETIR1803210 J Emerg Technol Innov Res*, 5
- Naranthatta S, Janardhanan P, Pilankatta R, Nair SS (2021) Green synthesis of engineered CdS nanoparticles with reduced cytotoxicity for enhanced bioimaging application. *ACS Omega* 6:8646–8655. https://doi.org/10.1021/ACSOMEGA.1C00519/ASSET/IMAGES/LARGE/AOIC00519_0014.JPEG
- Pikula K, Mintcheva N, Kulinich SA et al (2020) Aquatic toxicity and mode of action of CdS and ZnS nanoparticles in four microalgae species. *Environ Res* 186:109513. <https://doi.org/10.1016/J.ENVRES.2020.109513>
- Pourali P, Yahyaei B, Afsharnezhad S (2018) Bio-synthesis of gold nanoparticles by *Fusarium oxysporum* and assessment of their conjugation possibility with two types of β -lactam antibiotics without any additional linkers. *Microbiology* 87:229–237. <https://doi.org/10.1134/S0026261718020108>
- Qin Z, Yue Q, Liang Y et al (2018) Extracellular biosynthesis of bio-compatible cadmium sulfide quantum dots using *Trametes versicolor*. *J Biotechnol* 284:52–56. <https://doi.org/10.1016/J.JBIOTEC.2018.08.004>
- Rai M, Bonde S, Golinska P et al (2021) *Fusarium* as a novel fungus for the synthesis of nanoparticles: mechanism and applications. *J Fungi* 7:139. <https://doi.org/10.3390/jof7020139>
- Reyes-Esparza J, Martínez-Mena A, Gutiérrez-Sancha I et al (2015) Synthesis, characterization and biocompatibility of cadmium sulfide nanoparticles capped with dextrin for in vivo and in vitro imaging application. *J Nanobiotechnol* 13:1–14. <https://doi.org/10.1186/S12951-015-0145-X/TABLES/1>
- Sakpirom J, Kantachote D, Siripattanakul-Ratpukdi S et al (2019) Simultaneous bioprecipitation of cadmium to cadmium sulfide nanoparticles and nitrogen fixation by *Rhodospseudomonas palustris* TN110. *Chemosphere* 223:455–464. <https://doi.org/10.1016/J.CHEMOSPHERE.2019.02.051>
- Sandoval-Cárdenas DI, Gómez-Ramírez M, Rojas-Avelizapa NG, Vidales-Hurtado MA (2017a) Synthesis of cadmium sulfide nanoparticles by biomass of *Fusarium oxysporum* f. sp. lycopersici. *J Nano Res* 46:179–191. <https://doi.org/10.4028/www.scientific.net/JNanoR.46.179>
- Sandoval-Cárdenas I, Gómez-Ramírez M, Rojas-Avelizapa NG (2017b) Use of a sulfur waste for biosynthesis of cadmium sulfide quantum dots with *Fusarium oxysporum* f. sp. lycopersici. *Mater Sci Semicond Process* 63:33–39. <https://doi.org/10.1016/j.mssp.2017.01.017>
- Saraiva MA (2020) Interpretation of α -synuclein UV absorption spectra in the peptide bond and the aromatic regions. *J Photochem Photobiol B Biol* 212:112022. <https://doi.org/10.1016/J.JPHOTOBIO.2020.112022>
- Shen C-H (2019) Detection and analysis of nucleic acids. *Diagn Mol Biol*. <https://doi.org/10.1016/B978-0-12-802823-0.00007-9>
- Shivashankarappa A, Sanjay KR (2020) *Escherichia coli*-based synthesis of cadmium sulfide nanoparticles, characterization, antimicrobial and cytotoxicity studies. *Braz J Microbiol* 51(51):939–948. <https://doi.org/10.1007/S42770-020-00238-9>
- Siddiqi KS, Rashid M, Rahman A et al (2018) Biogenic fabrication and characterization of silver nanoparticles using aqueous-ethanolic extract of lichen (*Usnea longissima*) and their antimicrobial activity. *Biomater Res* 22:1–9. <https://doi.org/10.1186/S40824-018-0135-9/TABLES/1>
- Spatolisano E, de Angelis AR, Pellegrini LA (2022) Middle scale hydrogen sulphide conversion and valorisation technologies: a review. *ChemBioEng Rev* 9:370–392. <https://doi.org/10.1002/CBEN.202100057>
- Subramaniam S, Kumarasamy S, Narayanan M et al (2022) Spectral and structure characterization of *Ferula assafoetida* fabricated silver nanoparticles and evaluation of its cytotoxic, and photocatalytic competence. *Environ Res* 204:111987. <https://doi.org/10.1016/J.ENVRES.2021.111987>
- Sukhanova A, Bozrova S, Gerasimovich E et al (2022) Dependence of quantum dot toxicity in vitro on their size, chemical composition, and surface charge. *Nanomater* 12:2734. <https://doi.org/10.3390/NANO12162734>
- Xu J, Hu R, Wang Q et al (2019) Extracellular biosynthesis of bio-compatible CdSe quantum dots. *IET Nanobiotechnol* 13:962–966. <https://doi.org/10.1049/IET-NBT.2018.5432>
- Yadav C, Surana K, Singh PK, Bhattacharya B (2019) An ultra-simple method for synthesis of violet CdS quantum dots at sub-room temperature. *J Nanosci Nanotechnol* 20:3935–3938. <https://doi.org/10.1166/JNN.2020.17496>

Yang X, Jia Z, Cheng X et al (2018) Synthesis of N-acetyl-L-cysteine capped Mn:doped CdS quantum dots for quantitative detection of copper ions. *Spectrochim Acta A Mol Biomol Spectrosc* 199:455–461. <https://doi.org/10.1016/J.SAA.2018.04.003>

Publisher's Note Springer Nature remains neutral with regard to jurisdictional claims in published maps and institutional affiliations.

Springer Nature or its licensor (e.g. a society or other partner) holds exclusive rights to this article under a publishing agreement with the author(s) or other rightsholder(s); author self-archiving of the accepted manuscript version of this article is solely governed by the terms of such publishing agreement and applicable law.